LETTER

doi:10.1038/nature12147

The bromodomain protein Brd4 insulates chromatin from DNA damage signalling

Scott R. Floyd[1,2], Michael E. Pacold[1,3,4], Qiuying Huang[1], Scott M. Clarke[1], Fred C. Lam[1], Ian G. Cannell[1], Bryan D. Bryson[1], Jonathan Rameseder[1], Michael J. Lee[1], Emily J. Blake[1], Anna Fydrych[1], Richard Ho[1], Benjamin A. Greenberger[1], Grace C. Chen[1], Amanda Maffa[1], Amanda M. Del Rosario[1], David E. Root[5], Anne E. Carpenter[5], William C. Hahn[5,6], David M. Sabatini[4,5], Clark C. Chen[6,7], Forest M. White[1,8], James E. Bradner[5,6] & Michael B. Yaffe[1,5,7,8,9]

DNA damage activates a signalling network that blocks cell-cycle progression, recruits DNA repair factors and/or triggers senescence or programmed cell death[1]. Alterations in chromatin structure are implicated in the initiation and propagation of the DNA damage response[2]. Here we further investigate the role of chromatin structure in the DNA damage response by monitoring ionizing-radiation-induced signalling and response events with a high-content multiplex RNA-mediated interference screen of chromatin-modifying and -interacting genes. We discover that an isoform of Brd4, a bromodomain and extra-terminal (BET) family member, functions as an endogenous inhibitor of DNA damage response signalling by recruiting the condensin II chromatin remodelling complex to acetylated histones through bromodomain interactions. Loss of this isoform results in relaxed chromatin structure, rapid cell-cycle checkpoint recovery and enhanced survival after irradiation, whereas functional gain of this isoform compacted chromatin, attenuated DNA damage response signalling and enhanced radiation-induced lethality. These data implicate Brd4, previously known for its role in transcriptional control, as an insulator of chromatin that can modulate the signalling response to DNA damage.

Detection and repair of damaged DNA is integral for cell survival and accurate transmission of genetic information to progeny. Defects in the DNA damage response (DDR) contribute to oncogenesis and genomic instability in tumours[3,4] and render tumour cells sensitive to DNA-damaging cancer therapy[5]. Early signalling events that trigger and transduce the DDR occur in the context of chromatin, and it is likely that modulation of chromatin structure plays a role in DDR signalling[2]. Histone proteins are known targets of DDR post-translational modification[2,6], but a detailed understanding of the role of chromatin modulation in the DDR is lacking.

To explore the role of chromatin modulation in the DDR, we developed a high-throughput, high-content quantitative microscopy assay multiplexed for early and late DDR endpoints, and applied this to an RNA-mediated interference (RNAi) library focused on proteins that interact with and modify chromatin (see Methods)[7,8]. For each time point, cells were co-stained with γH2AX antibodies to measure early signalling events in the DDR, Hoechst 33342 to monitor cell-cycle progression and phospho-histone H3 (pHH3) to measure mitotic entry. At the latest time point, cleaved caspase-3 (CC3) was substituted for pHH3 to measure apoptotic cell death. The screening assay was validated with small molecule inhibitors of DDR signalling as well as RNAi directed against known components of the DDR pathway (Supplementary Figs 1–4).

The most pronounced increase in γH2AX foci number, size and intensity after ionizing radiation was observed at 1 and 6 h after knockdown of Brd4; this remained elevated at 24 h (Fig. 1a, b and Supplementary Fig. 4). Eight hairpins directed against Brd4 showed this effect, making off-target effects unlikely (Fig. 1a and Supplementary Fig. 4). Neither Brd4 knockdown in the absence of irradiation (Fig. 1b) nor knockdown of other bromodomain-containing proteins (Figs 1b and Supplementary Fig. 4) significantly altered γH2AX. Increased ionizing-radiation-induced γH2AX after Brd4 loss was further confirmed using short interfering RNA (siRNA) oligonucleotides targeting additional independent Brd4 sequences (Fig. 1f and Supplementary Fig. 5).

Brd4 encodes three splice isoforms (A, B and C in Fig. 1c). Each isoform contains two amino (N)-terminal bromodomains (BD1 and BD2) that bind acetylated lysine, and an extra-terminal (ET) domain recently reported to interact with several chromatin-binding proteins[9]. The A isoform contains a carboxy (C)-terminal domain (CTD) that functions as a transcriptional co-activator with the pTEFb complex[10,11]. This region is notably absent in the B and C isoforms, and in the B isoform it is replaced with a divergent short 75 amino-acid segment. All three Brd4 isoforms are expressed in U2OS cells, and the short hairpin RNAs (shRNAs) used in our screen targeted all three isoforms (Supplementary Table 1). We confirmed that a single distinct siRNA that was active against all Brd4 isoforms replicated the Brd4 loss-of-function phenotype of elevated ionizing-radiation-induced γH2AX (Supplementary Fig. 5).

To establish the relative effects of the isoforms on the DDR, we performed gain-of-function experiments. Overexpression of Brd4 isoform B most potently suppressed ionizing-radiation-induced γH2AX foci (Fig. 1d). We designed isoform-specific siRNAs to reduce expression of isoform A or B messenger RNA (mRNA) (Fig. 1e) and protein (Supplementary Fig. 5) selectively; selective targeting of isoform C was not technically possible owing to complete coding sequence overlap with isoforms A and B. We observed that selective depletion of Brd4 isoform B, but not isoform A, increased H2AX phosphorylation over a wide range of ionizing radiation doses (Fig. 1f).

To investigate whether elevated γH2AX levels observed in Brd4-deficient cells resulted from increased production of ionizing-radiation-induced DNA double-strand breaks or from faulty double-strand break repair, we used pulsed-field gel electrophoresis to quantify double-strand breaks in control and Brd4 knockdown cells. As shown in Fig. 2a, Brd4 knockdown had minimal effects on the generation and repair kinetics of double-strand breaks. These observations, together with our finding that individual γH2AX foci were larger and more intense in irradiated Brd4 knockdown cells (Fig. 1b, Supplementary Fig. 4 and Supplementary Tables 1 and 2), indicate that there is enhanced signalling from damaged DNA in the absence of Brd4, rather than an increase in the amount of damage or repair deficiency.

[1]Koch Institute for Integrative Cancer Research, Massachusetts Institute of Technology, Cambridge, Massachusetts 02139, USA. [2]Department of Radiation Oncology, Beth Israel Deaconess Medical Center, Boston, Massachusetts 02215, USA. [3]Department of Radiation Oncology, Dana-Farber Cancer Institute, Boston, Massachusetts 02215, USA. [4]Whitehead Institute, Cambridge, Massachusetts 02139, USA. [5]Broad Institute of Harvard and MIT, Cambridge, Massachusetts 02142, USA. [6]Department of Medical Oncology, Dana-Farber Cancer Institute, Boston, Massachusetts 02215, USA. [7]Department of Surgery, Beth Israel Deaconess Medical Center, Boston, Massachusetts 02215, USA. [8]Department of Biological Engineering, Massachusetts Institute of Technology, Cambridge, Massachusetts 02139, USA. [9]Department of Biology, Massachusetts Institute of Technology, Cambridge, Massachusetts 02139, USA.

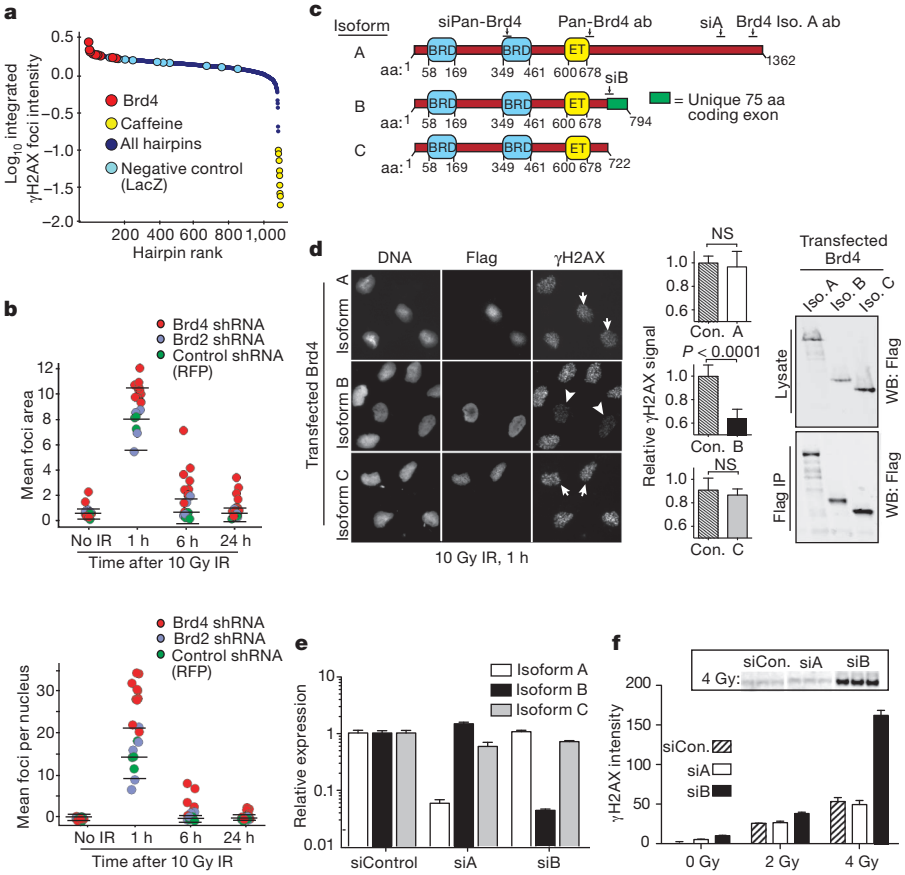

Figure 1 | Brd4 isoform B suppresses H2AX phosphorylation after ionizing radiation. **a**, Rank of hairpins from shRNA screen ordered by integrated γH2AX foci intensity at 1 h after 10 Gy ionizing radiation (details of screening assay in Supplementary Figs 1–4). **b**, γH2AX foci size (upper panel) and mean γH2AX foci per nucleus (lower panel) after 10 Gy ionizing radiation (IR) from cells expressing indicated shRNAs (bars show mean and two standard deviations of control values). RFP, red fluorescent protein. **c**, Domain structure of Brd4 isoforms showing conserved tandem bromodomains (BRD), extra-terminal (ET) domain, siRNA and antibody target sequences, and unique isoform B exon. aa, amino acid; Iso., isoform. **d**, H2AX phosphorylation in cells expressing Flag-tagged Brd4 isoform B (arrowheads) or A and C (arrows) at 1 h after 10 Gy IR. Left: representative images. Middle: quantification of 10 fields from two independent experiments with mean γH2AX signal normalized to untransfected cells. Right: immunoblot of isoform expression levels in whole-cell lysates and anti-Flag immunoprecipitates. Con., control. **e**, Isoform-specific Brd4 knockdown in cells transfected with the indicated siRNA and analysed by quantitative real-time PCR with reverse transcription ($n = 3$). **f**, H2AX phosphorylation levels 1 h after indicated ionizing radiation exposure in cells transfected with isoform-specific siRNA ($n = 3$). Inset shows representative immunoblot for triplicate samples. Data are from U2OS cells. Error bars, s.e.m.; *P* values were determined using Student's *t*-test in this and all subsequent figures unless otherwise indicated.

Changes in overall chromatin structure can affect H2AX phosphorylation, probably by controlling the accessibility of signalling molecules to DNA damage sites[12,13]. Interestingly, γH2AX foci form more readily in 'open' areas of euchromatin[14], histone acetylation has been linked to the 'open' chromatin state and histone deacetylase inhibitors are known to increase H2AX phosphorylation[15]. We speculated that a bromodomain protein could influence H2AX phosphorylation through interaction with acetylated histones and effects on global chromatin structure, and therefore performed micrococcal nuclease susceptibility experiments. Knockdown of Brd4 isoform B increased digestion by micrococcal nuclease, indicating a more 'open' overall chromatin structure, whereas knockdown of isoform A had minimal effects (Fig. 2b). Furthermore, we observed that cells transfected with Brd4 isoform B showed a distinct nuclear 4′,6-diamidino-2-phenylindole (DAPI) staining pattern, indicating a change in chromatin structure (Fig. 2c). As shown in Fig. 2d, e, quantification of the

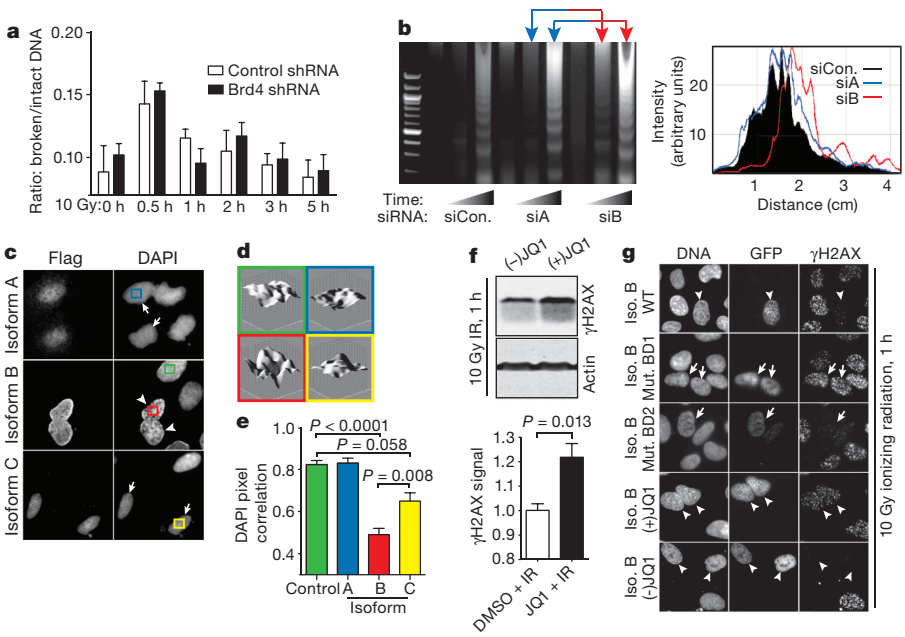

Figure 2 | Brd4 isoform B limits H2AX phosphorylation through bromodomain-acetyl lysine-mediated effects on chromatin structure. **a**, Pulsed-field electrophoresis analysis of DNA from stable cell lines expressing indicated shRNA after 10 Gy IR ($n = 3$). **b**, Left: micrococcal nuclease assay of control or Brd4 knockdown cells. Right: line traces of representative gel lanes. **c**, Chromatin structure from cells expressing Flag-tagged Brd4 isoform B (arrowheads) or A and C (arrows) shown by DAPI staining. **d**, Three-dimensional representation of nuclear DAPI staining intensity from cells in **c** as indicated by coloured frames. **e**, DAPI pixel correlation from Brd4 isoform A, B, C and untransfected control cells ($n = 3$). **f**, Immunoblots (top) and quantification (bottom) of H2AX phosphorylation after 250 nM DMSO, or active (+) and inactive (−) JQ1 at 1 h after 10 Gy ionizing radiation ($n = 3$). **g**, γH2AX signal 1 h after 10 Gy IR in cells expressing green fluorescent protein (GFP)–wild-type Brd4 isoform B (arrowheads), isoform B with mutations that abrogate acetyl lysine binding of bromodomain 1 (BD1) or 2 (BD2) (arrows), or wild-type Brd4 isoform B in the presence of 250 nM (−) JQ1 (inactive) or (+) JQ1 as indicated.

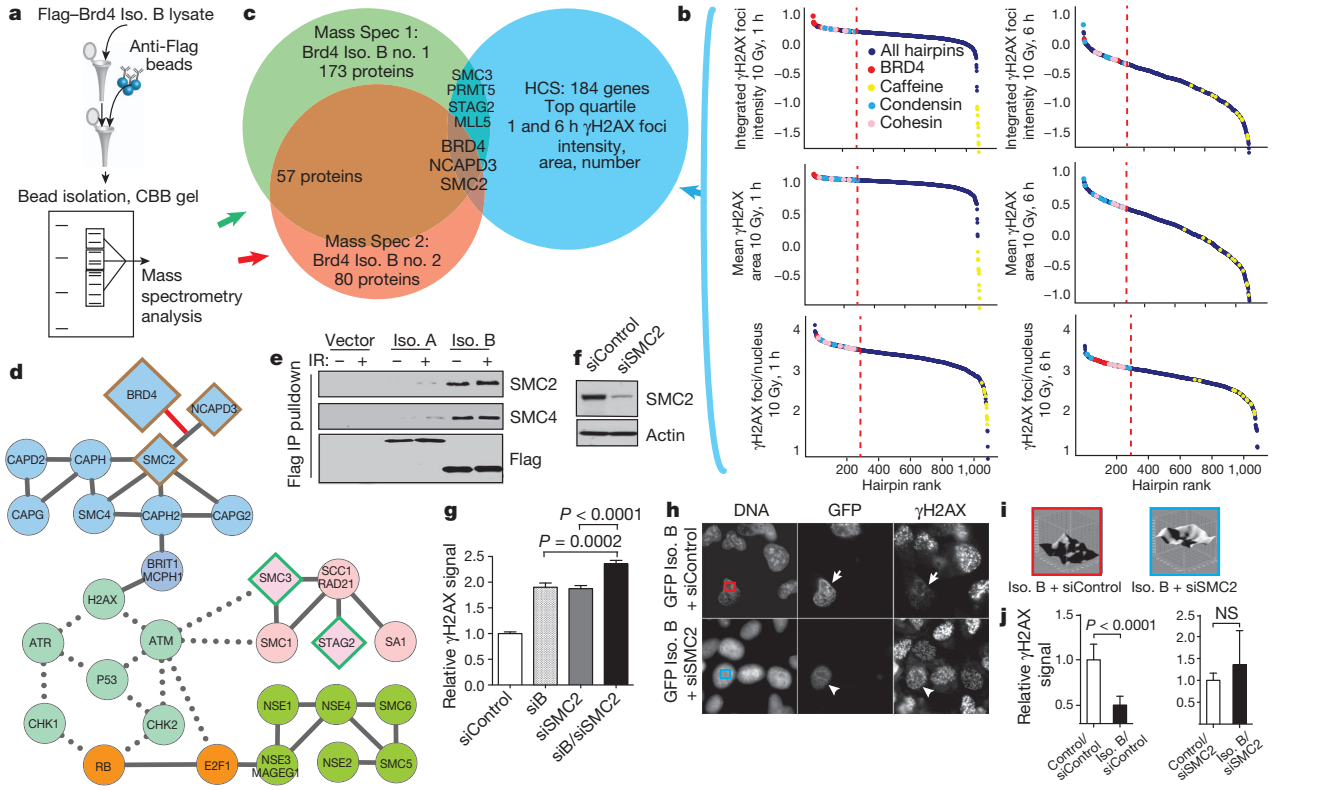

Figure 3 | Brd4 isoform B interaction with the condensin complex affects H2AX phosphorylation. **a**, Mass spectrometry identification of co-immunoprecipitated proteins from Flag-tagged Brd4 isoform-B-expressing cells. **b**, Identification of candidate Brd4 interactors by ranking chromatin modifier shRNAs from screen for elevated H2AX foci intensity, area and number at 1 and 6 h after 10 Gy IR. Dashed red lines indicate top quartile. **c**, Intersection of two independent mass-spectrometry experiments (**a**) with the top quartile of candidates in **b**. Overlapping set includes Brd4, SMC2 and NCAPD3. **d**, Network representation of SMC proteins and relation to DNA damage signalling with protein–protein and kinase–substrate interactions collated from the literature. Protein–protein and kinase–substrate interactions shown by solid and dotted lines, respectively. Colours indicate condensin complex (blue), cohesin complex (pink), other SMC protein complexes (green), cell-cycle regulators (orange) and DNA damage signalling machinery (mint). Diamonds show mass spectrometry and high-content screening hits from **a** and **b**. Border colours denote overlap of screens from **c**. The new interaction of Brd4 with the condensin complex is indicated by the red line. **e**, Validation of isoform-B–condensin interaction with blotting immunoprecipitates from cells transfected with indicated Flag-tagged constructs. **f**, Immunoblot verification of SMC2 knockdown from cells transfected with SMC2 siRNA. **g**, Nuclear γH2AX signal from cells transfected with indicated combinations of control DNA, Brd4 isoform B and/or SMC2 siRNA. Data were quantified from ten fields of two independent experiments normalized to control cells. **h**, H2AX phosphorylation 1 h after 10 Gy IR in cells simultaneously expressing isoform B and control (arrows) or SMC2 siRNA (arrowheads). **i**, Chromatin staining pattern in cells simultaneously expressing isoform B and control (red frame) or SMC2 (blue frame) siRNA. **j**, Mean nuclear γH2AX signal in GFP–isoform-B-expressing cells with or without SMC2 knockdown. Data are from ten fields of two independent experiments, as in **h**, normalized to control untransfected cells.

nuclear staining texture showed a more heterogeneous DAPI intensity pattern, and significantly lower pixel-to-pixel correlation of DAPI staining in cells overexpressing isoform B, indicative of isoform-B-mediated alterations in global chromatin structure. Expression of isoform A had no effect on DAPI staining, whereas overexpression of isoform C had smaller effects than those observed with isoform B.

Our finding that Brd4 isoform B expression affects global chromatin structure and attenuates H2AX phosphorylation in response to DNA damage led us to investigate the subcellular localization of isoform B in response to ionizing radiation. Immunofluorescence experiments showed that ionizing radiation did not grossly alter Brd4 isoform B nuclear localization, which tightly mirrored DNA patterns shown by DAPI staining (Supplementary Fig. 6a). Interestingly, subcellular fractionation of U2OS cells and extraction of chromatin-bound proteins demonstrated that irradiation caused enhanced isoform B association with the high salt-extractable chromatin fraction (Supplementary Fig. 6b, c), indicating increased association of isoform B with chromatin after DNA damage.

Bromodomains recognize epigenetic marks on chromatin by binding to acetyl-lysine[16]. We therefore tested the contribution of Brd4 bromodomain interactions to alterations in γH2AX phosphorylation using JQ1, a small molecule inhibitor of BET bromodomains[17]. Only the active enantiomer of JQ1 caused increased H2AX phosphorylation after irradiation in U2OS cells (Fig. 2f), similar to the effects observed after Brd4 isoform-B-specific knockdown. Furthermore, JQ1 treatment or Brd4 isoform B knockdown did not significantly alter total histone levels or levels of histone acetylation (Supplementary Figs 7 and 8). Interestingly, overexpression of Brd4 isoform B led to alteration in the nuclear staining pattern of acetyl-lysine, closely mirroring the DAPI staining pattern induced by expression of isoform B (Supplementary Fig. 7b).

The concentration of JQ1 that we used (250 nM) is consistent with the reported *in vitro* half-maximum inhibitory concentration for Brd4 bromodomains 1 (BD1, 77 nM) and 2 (BD2, 33 nM)[17]. To evaluate directly the role of each bromodomain in isoform B, we performed gain-of-function experiments using wild-type Brd4 in the absence or presence of JQ1, or constructs harbouring mutations that abrogate acetyl lysine binding by BD1 or BD2. Mutations in BD1, or addition of the active enantiomer of JQ1, potently reversed the γH2AX-suppressive effects of isoform B expression (Fig. 2g). Notably, mutations that abrogate BD1 binding to acetyl-lysine also rescued the ionizing-radiation-induced cell death phenotype observed with Brd4 isoform B gain-of-function (see below), implicating BD1 in the mechanism of DNA damage inhibition (cf. Fig. 4b).

To probe further the role of lysine acetylation on γH2AX-Brd4 effects, we examined the combined effects of histone deacetylase

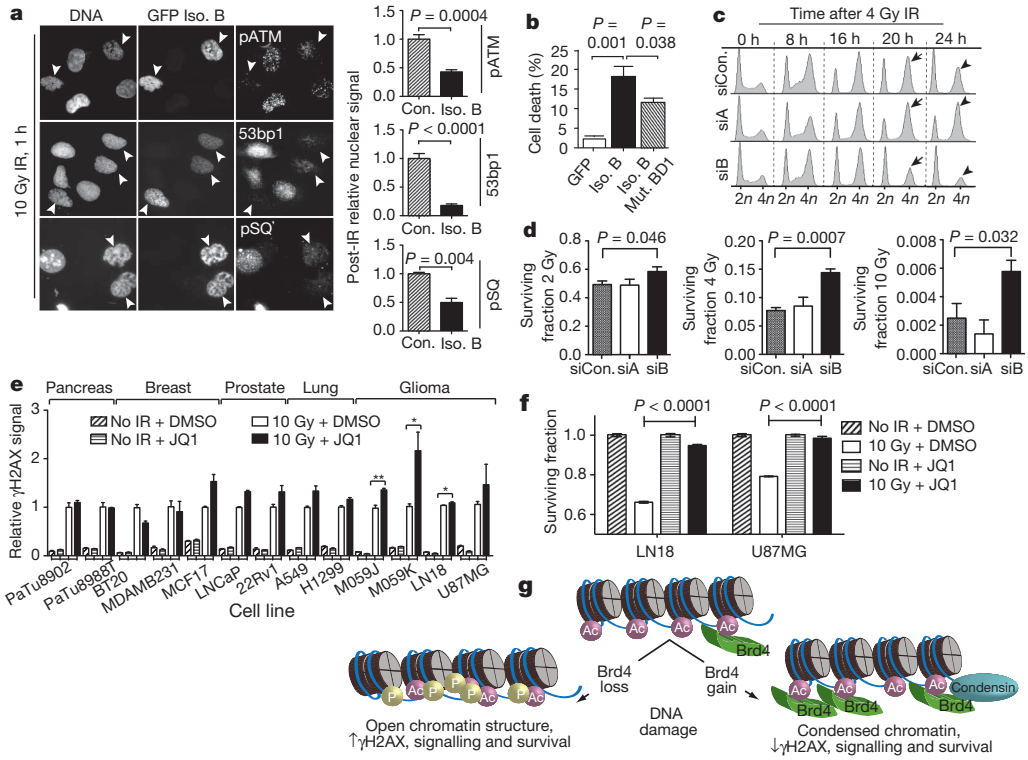

Figure 4 | Brd4 isoform B affects ionizing-radiation-induced cell-cycle checkpoints and survival. **a**, Loss of DNA damage signalling in cells expressing Brd4 isoform B. Left: representative images stained for indicated DDR proteins 1 h after 10 Gy IR. Arrowheads indicate isoform-B-expressing cells. Right: quantification of ten representative fields from two independent experiments normalized to untransfected cells. **b**, Cell death 24 h after 10 Gy IR in cells expressing wild-type or bromodomain-1-mutant isoform B (Isoform B mut. BD1) scored for cleaved caspase 3 by flow cytometry ($n = 3$). **c**, Ionizing-radiation-induced cell-cycle arrest and recovery in Brd4 isoform knockdown cells assayed by propidium iodide staining and flow cytometry. **d**, Cell survival after irradiation in Brd4 isoform knockdown cells measured by colony formation. **e**, JQ1 effect on γH2AX in several human cancer cell types commonly treated with radiotherapy. No IR, no ionizing radiation. **f**, Radiation survival effects of JQ1 in glioma cell lines measured at 72 h by CellTiterGlo ($n = 3$). **g**, Model for Brd4 effects on DNA damage signalling.

inhibitors and Brd4 knockdown. We found that when Brd4 isoform B knockdown was combined with exposure to 50 nM LBH589, an inhibitor of histone deacetylases 1–3 and 6 (ref. 18), H2AX phosphorylation was enhanced to a greater extent than with either treatment alone (Supplementary Fig. 9). This effect could be observed even in unirradiated cells, although the total amount of H2AX phosphorylation remained lower than that seen in irradiated cells. Taken together, these findings indicate that Brd4 isoform B binding to acetylated regions of chromatin alters chromatin structure and limits H2AX phosphorylation.

Brd4 also has a defined role in transcriptional modulation, largely through interactions of isoform A with the pTEFb transcriptional complex[10,11]. To investigate the contribution of Brd4-driven transcriptional changes to the suppression of DNA damage signalling, we profiled mRNA expression patterns of cells stably expressing control or Brd4 shRNAs. Only one DDR-associated transcript, CHEK2, showed a differential expression change of twofold or more (Supplementary Fig. 10a). Importantly, transient Brd4 knockdowns with siRNA, or short-term inhibition with JQ1, both of which increased γH2AX foci formation after irradiation (Supplementary Fig. 5a and Fig. 2f), caused no change in CHEK2 mRNA levels (Supplementary Fig. 10b, c), and neither long-term nor short-term Brd4 knockdown affected the protein levels of several DDR molecules, including Chk2 (Supplementary Fig. 10d). Moreover, the suppression of DDR signalling by Brd4 isoform B overexpression was insensitive to transcription and translation inhibition with α-amanitin and cycloheximide, respectively (Supplementary Fig. 11).

As interactions between Brd4 and other protein complexes involved in modulating chromatin structure were probably responsible for the DDR effects we observed, we identified proteins co-immunoprecipitated with isoform B after DNA damage using mass spectrometry (Fig. 3a and Supplementary Fig. 12). From two independent experiments, we obtained a common set of 57 interacting proteins (Supplementary Tables 3 and 4). Because the DDR-relevant Brd4-binding proteins presumably function in the same pathway as Brd4, we reasoned that loss of these proteins should show a phenotype similar to Brd4 loss-of-function. We therefore used our existing high-content screening data to create a list of the top quartile of genes ranked by increased γH2AX foci intensity, number and size at 1 and 6 h after irradiation (Fig. 3b). The overlap of this list with the list of isoform-B-interacting proteins showed two members of the condensin II complex, SMC2 and CAPD3 (Fig. 3c, d). This finding was intriguing as the condensin II complex has a known role in chromatin compaction in both mitotic and interphase cells, and has been linked to DNA damage repair[19]. We performed immunoprecipitation experiments after DNA damage, and found that the SMC2 and SMC4 components of the condensin II complex co-immunoprecipitated with Brd4 isoform B, whereas Brd4 isoform A had minimal co-association (Fig. 3e). To verify the role of this interaction on the γH2AX effects we observed, we performed combined isoform B and SMC2 knockdown and assayed H2AX phosphorylation 24 h after siRNA transfection, when knockdown of each protein is sub-maximal. We found that H2AX phosphorylation was enhanced with combined knockdown over knockdown of either protein alone (Fig. 3f, g). Furthermore, in cells overexpressing isoform B, SMC2 knockdown could abrogate the suppressive effects of Brd4 on γH2AX, demonstrating a functional interaction between isoform B and the condensin II complex in modulating γH2AX (Fig. 3h, j). Finally, we noted that the effects of isoform B on the DAPI staining pattern of chromatin were abrogated by co-transfection of SMC2 siRNA, indicating that the Brd4-condensin II interaction is involved in chromatin structure alterations (Fig. 3i).

We next investigated isoform B effects on other components of the DDR. We found that isoform B gain-of-function inhibited ionizing-radiation-induced foci formation of several other known DDR signalling components including 53BP1, phosphorylated ATM and several DDR signalling molecules containing the phospho-SQ DDR kinase substrate motif (Fig. 4a). In addition, overexpression of isoform B resulted in increased cell death after irradiation, an effect that was significantly diminished by mutation of BD1 (Fig. 4b). The cell death observed in Brd4 isoform B overexpressing cells seems to result from mitotic catastrophe, consistent with a loss of DDR signalling that results in failed cell-cycle arrest (Supplementary Fig. 13). We also investigated the effect of isoform B knockdown on DDR-induced cell-cycle arrest and survival. Interestingly, isoform B loss-of-function

allowed increased cell survival with more rapid and efficient recovery from cell-cycle arrest after irradiation, complementing the inverse findings observed with isoform B gain-of-function (Fig. 4c, d).

Given the effects of Brd4 isoform B on ionizing-radiation-induced DDR signalling and survival, we considered that isoform B might have a role in tumour responses to irradiation. We screened a panel of established cell lines from several human tumour types commonly treated with radiotherapy for γH2AX effects using the JQ1 inhibitor. Several cell types showed increased ionizing-radiation-induced H2AX phosphorylation with JQ1 treatment, including breast, prostate and particularly glioma cancer cell lines (Fig. 4e). Just as we had observed with U2OS cells, irradiation had the expected killing effect on dimethylsulphoxide (DMSO)-treated glioma cells; however, this killing effect was markedly reduced in JQ1-treated glioma cells, consistent with our finding of increased DDR signalling and radioresistance with decreased Brd4 function (Fig. 4f). Conversely, overexpression of Brd4 isoform B in glioma cells inhibited H2AX phosphorylation, consistent with decreased DDR signalling upon Brd4 gain-of-function (Supplementary Fig. 14).

We conclude that structural alterations in chromatin mediated by Brd4 acetyl lysine binding function to attenuate the DNA damage signalling response to ionizing radiation. These effects on DDR signalling are consistent with the induction of a chromatin structure that is inhibitory to the formation of γH2AX in the case of higher levels of Brd4 isoform B expression, or a more 'open' chromatin structure that facilitates γH2AX foci formation when Brd4 expression is reduced, or after pharmacological inhibition of bromodomain binding (shown schematically in Fig. 4g).

Our data indicate that Brd4 affects DDR signalling through mechanisms distinct from known transcriptional interactions with the P-TEFb transcriptional complex. The relevant Brd4 isoform that modulates the DDR, isoform B, lacks the pTEFb-interacting region. In addition, chemical inhibition of transcription/translation had no effect on the ability of Brd4 to suppress DDR-induced γH2AX. This finding is in line with the recent identification of other chromatin-interacting proteins such as KAP-1 and Brg1 that have roles in DNA damage signalling that do not seem to arise directly from the transcriptional activity that these molecules also possess[13,20]. Rather, the enhancement of several parameters of γH2AX foci after Brd4 knockdown, including their size and intensity, in addition to their number, point to a role for Brd4 in limiting the propagation of DDR signalling after ionizing radiation. This effect seems to involve the recruitment of a chromatin-condensing complex to sites of acetylation, a new role for Brd4. In agreement with this, overexpression of Brd4, even in the absence of damage, resulted in alterations of chromatin structure and nuclear acetylation patterns, consistent with a model of Brd4 isoform B binding to and occluding acetyl-lysine sites on chromatin and recruiting chromatin compaction machinery. These findings implicate bromodomain-mediated interactions in modulating specific chromatin structures that inhibit the propagation of DDR signalling in chromatin[12,15], and indicate that Brd4 isoform B alters the threshold response of γH2AX to DNA damage.

METHODS SUMMARY

Image-based high-content screening was performed in 384-well plate format using an arrayed lentiviral shRNA library from The RNAi Consortium. Screen images were acquired with a Cellomics microscope (Thermo Scientific) and quantified using CellProfiler software. siRNAs and antibodies were from commercial sources. We used Affymetrix U133 Plus 2.0 arrays for expression profiling. Mass spectrometry data from Brd4 immunoprecipitates after SDS–PAGE was acquired with an Orbitrap XL instrument (Thermo Scientific), and data analysed with Mascot software. Interactions for network analysis were hand-curated from primary literature using the keywords 'DNA damage', 'cell cycle checkpoint', 'chromatin structure', 'ATM/ATR', 'Chk1/Chk2' and 'SMC proteins'. Further details are provided in the Methods.

Full Methods and any associated references are available in the online version of the paper.

Received 19 July 2011; accepted 3 April 2013.
Published online 2 June 2013.

1. Jackson, S. P. & Bartek, J. The DNA-damage response in human biology and disease. *Nature* **461,** 1071–1078 (2009).
2. Misteli, T. & Soutoglou, E. The emerging role of nuclear architecture in DNA repair and genome maintenance. *Nature Rev. Mol. Cell Biol.* **10,** 243–254 (2009).
3. Gorgoulis, V. G. *et al.* Activation of the DNA damage checkpoint and genomic instability in human precancerous lesions. *Nature* **434,** 907–913 (2005).
4. Bartkova, J. *et al.* DNA damage response as a candidate anti-cancer barrier in early human tumorigenesis. *Nature* **434,** 864–870 (2005).
5. Kastan, M. B. & Bartek, J. Cell-cycle checkpoints and cancer. *Nature* **432,** 316–323 (2004).
6. Polo, S. E. & Jackson, S. P. Dynamics of DNA damage response proteins at DNA breaks: a focus on protein modifications. *Genes Dev.* **25,** 409–433 (2011).
7. Moffat, J. *et al.* A lentiviral RNAi library for human and mouse genes applied to an arrayed viral high-content screen. *Cell* **124,** 1283–1298 (2006).
8. Carpenter, A. E. *et al.* CellProfiler: image analysis software for identifying and quantifying cell phenotypes. *Genome Biol.* **7,** R100 (2006).
9. Rahman, S. *et al.* The Brd4 extraterminal domain confers transcription activation independent of pTEFb by recruiting multiple proteins, including NSD3. *Mol. Cell. Biol.* **31,** 2641–2652 (2011).
10. Yang, Z. *et al.* Recruitment of P-TEFb for stimulation of transcriptional elongation by the bromodomain protein Brd4. *Mol. Cell* **19,** 535–545 (2005).
11. Jang, M. K. *et al.* The bromodomain protein Brd4 is a positive regulatory component of P-TEFb and stimulates RNA polymerase II-dependent transcription. *Mol. Cell* **19,** 523–534 (2005).
12. Murga, M. *et al.* Global chromatin compaction limits the strength of the DNA damage response. *J. Cell Biol.* **178,** 1101–1108 (2007).
13. Ziv, Y. *et al.* Chromatin relaxation in response to DNA double-strand breaks is modulated by a novel ATM- and KAP-1 dependent pathway. *Nature Cell Biol.* **8,** 870–876 (2006).
14. Cowell, I. G. *et al.* γH2AX foci form preferentially in euchromatin after ionising-radiation. *PLoS ONE* **2,** e1057 (2007).
15. Kim, J. A., Kruhlak, M., Dotiwala, F., Nussenzweig, A. & Haber, J. E. Heterochromatin is refractory to γ-H2AX modification in yeast and mammals. *J. Cell Biol.* **178,** 209–218 (2007).
16. Filippakopoulos, P. *et al.* Histone recognition and large-scale structural analysis of the human bromodomain family. *Cell* **149,** 214–231 (2012).
17. Filippakopoulos, P. *et al.* Selective inhibition of BET bromodomains. *Nature* **468,** 1067–1073 (2010).
18. Bradner, J. E. *et al.* Chemical phylogenetics of histone deacetylases. *Nature Chem. Biol.* **6,** 238–243 (2010).
19. Wu, N. & Yu, H. The Smc complexes in DNA damage response. *Cell Biosci.* **2,** 5 (2012).
20. Lee, H.-S., Park, J.-H., Kim, S.-J., Kwon, S.-J. & Kwon, J. A cooperative activation loop among SWI/SNF, γ-H2AX and H3 acetylation for DNA double-strand break repair. *EMBO J.* **29,** 1434–1445 (2010).

Supplementary Information is available in the online version of the paper.

Acknowledgements We thank H. Le, T.R. Jones and M. Vokes for assistance with screening and image analysis. We thank C. Whittaker, S. Hoersch and M. Moran for computing and data analysis assistance; C. Reinhardt, C. Ellson and A. Gardino for manuscript editing; and P. Filippakopoulos and S. Knapp for discussions. This work was partially supported by the Koch Institute and Center for Environmental Health Sciences National Institutes of Health Core Grants P30-CA14051 and ES-002109; and by grants R01-ES15339, 1-U54-CA112967-04 and R21-NS063917; a SPARC grant to M.B.Y.; and a Holman Pathway Research Resident Seed Grant, American Society for Radiation Oncology Junior Faculty Career Research Training Award, Klarman Scholar, Koch Institute Clinical Investigator Award, and Burroughs Wellcome Career Award for Medical Scientists to S.R.F.

Author Contributions S.R.F. and M.B.Y. designed the study, supervised the experiments, analysed the data and wrote the manuscript. D.E.R., W.C.H. and D.M.S. were involved in the design and preparation of the lentiviral shRNA library. S.R.F., M.E.P. and E.B. performed the image-based high-content screen and initial analysis. A.E.C. aided in digital image analysis. S.R.F., Q.H., S.M.C., F.C.L., I.G.C., M.J.L., A.F., R.H., B.A.G., G.C.C. and A.M. performed biochemical, cell biological and molecular biological experiments. B.D.B., A.M.D. and F.M.W. performed mass spectrometry experiments and analysis. J.R. performed bioinformatics analysis. J.E.B. contributed JQ1 compounds and cell lines. S.R.F. and M.B.Y. designed and supervised the experiments. C.C.C., J.E.B. and F.M.W. contributed to the intellectual development of the study and technical writing of the manuscript. All authors contributed to editing the manuscript.

Author Information The expression profiling Affymetrix u133 plus dataset has been deposited in the NCBI Gene Expression Omnibus database under accession number GSE30700. Reprints and permissions information is available at www.nature.com/reprints. The authors declare no competing financial interests. Readers are welcome to comment on the online version of the paper. Correspondence and requests for materials should be addressed to M.B.Y. (myaffe@mit.edu).

METHODS

Antibodies and stains. Mouse monoclonal antibodies against γH2AX were from Upstate/Millipore (catalogue number 05636), Actin (Sigma, catalogue number A5441), phospho-ATM Serine 1981 (Rockland, catalogue number 200-301-400), Flag (Sigma, catalogue number F3165), ornithine decarboxylase (Abcam, catalogue number ab66067), RAD50 (GeneTex, catalogue number GTX70228), NBS1 (Abcam, catalogue number ab49958), MDC1 (Novus, catalogue number NB100-396) and Lamin (Millipore, catalogue number 05-714). Rabbit polyclonal and monoclonal antibodies against Brd4 were from Abcam (catalogue number Ab46199) and Pan-Brd4 from Sigma (catalogue number AV39076), 53BP1 (Novus, catalogue number NB100-304), CHEK2 (Cell Signaling Technology, catalogue number 2662), total H2AX (Abcam, catalogue number ab11175), phospho-SQ (Cell Signaling Technology, catalogue number 2851), MRE11 (Novus, catalogue number NB100-142), cleaved caspase 3 (Cell Signaling Technology, catalogue number 9664), SMC2 (Cell Signaling Technology, catalogue number 5329), SMC4 (Cell Signaling Technology, catalogue number 5547), phopho-histone H3 (Upstate/Millipore, catalogue number 06570 and BD/Pharmingen catalogue number 559565). DNA stains were Hoechst 33342 (Invitrogen, catalogue number H1399) propidium iodide (Invitrogen, catalogue number P1304MP) and ethidium bromide (Invitrogen, catalogue number 15585011). Fluorescent antibodies were from Invitrogen: goat anti-rabbit and goat anti-mouse Alexa 488, 555 and 647 (catalogue numbers A11001, A21422, A21235, A21238, A21428 and A21244).

Small molecule inhibitors. Brd4 bromodomain inhibitor (+)JQ1 and its inactive enantiomer (−)JQ1 were synthesized as described[17] and were used at 250 nM. α-Amanitin (catalogue number A2263) and cycloheximide (catalogue number C4859) were from Sigma and were used at concentrations as indicated (α-amanitin 1–16 μM; cycloheximide 35–560 μM). UCN01 was from Sigma (catalogue number U6508) and was used at concentrations of 0.003–10 μM. Caffeine was from Sigma (catalogue number C0750) and was used at concentrations of 10–25 mM. LBH589 was a gift from J. Bradner).

RNAi library. shRNA was applied to cells using a high-titre arrayed lenti-viral library maintained in the pLKO_TRC001 vector as described[7].

Image-based screens. For shRNA screens and small molecule tests, human U2OS osteosarcoma cells (ATCC HTB-96) were grown in DMEM + Pen/Strep + 10% v/v FBS (complete media) at 37 °C in a 5% CO_2 atmosphere. All screens were performed at passage 10–15. Cells were tested for mycoplasma by PCR before seeding and infection. U2OS cells were seeded with a MicroFill (Biotek) in 384-well black, clear bottom plates (Greiner) at a density of 300 (shRNA) cells per well in 50 μl of media, and allowed to attach overnight at 37 °C in a 5% CO_2 atmosphere. For shRNA screens, the media was exchanged the following day to complete media with 8 μg ml^{-1} polybrene using a JANUS workstation (PerkinElmer). Virus infection was performed on an EP3 workstation (PerkinElmer) with 1.5 μl of high-titre retrovirus. All plates had two wells infected with 1.5 μl of control virus with shRNA directed against H2AX. Plates were centrifuged in a swinging-bucket rotor at 1180*g* for 30 min after infection and returned to the incubator overnight. The plates were then selected with 2.5 μg ml^{-1} puromycin for 48 h, and allowed to proliferate in complete media for another 48 h, with media exchanges performed on the JANUS or RapidPlate (Qiagen) liquid handling workstations. Eight wells in each plate were not selected with puromycin. For small molecule testing, cells were plated at 500 cells per well in 384-well plates. The day after plating, small molecules at different concentrations in 100 nl DMSO were pin transferred to cells with a CyBio robot, and cells were propagated for 16 h. For both small molecule and shRNA screens, four plates were created in replicate for the time points outlined below. Four wells were left untreated in each plate, and received 25 mM caffeine in complete media 1 h before irradiation. All plates were treated with 10 Gy of 667 keV X-rays from a ^{137}Cs source in a Gammacell irradiator (Atomic Energy of Canada). A 0 h control plate was not irradiated. The plates were returned to the incubator and fixed with 4.4% w/v paraformaldehyde in phosphate-buffered saline (PBS) at 1, 6 and 24 h after irradiation. Plates were stored in PBS at 4 °C before staining. Fixed plates were washed three times with PBS and blocked with 24 μl of GSDB (0.15% goat serum, 8.33% goat serum, 120 mM sodium phosphate, 225 mM NaCl) for 30 min. The 0, 1 and 6 h plates were incubated with 1:300 dilutions in GSDB of primary mouse monoclonal anti-γH2AX (Ser 139), and rabbit polyclonal anti-pHH3 antibody. For the 24 h plates, we substituted 1:300 rabbit polyclonal anti-cleaved caspase 3 for the pHH3 antibody. All plates were incubated overnight at 4 °C, washed and stained with a secondary antibody mix containing 10 μg ml^{-1} Hoescht 33342, 1:300 goat anti-mouse polyclonal-Alexa Fluor 488 and goat anti-rabbit polyclonal-Alexa Fluor 555 in GSDB. After a second overnight incubation at 4 °C, the plates were washed three times in PBS and stored in 50 μl per well 50 μM Trilox (Sigma) in PBS at 4 °C.

Imaging and image analysis. Plates were allowed to equilibrate to room temperature for 30 min and imaged on a Cellomics ArrayScan VTI automated microscope with a ×20 objective lens. The acquisition parameters were the same for each shRNA or chemical inhibitor. Six fields per well were imaged, with three channels/field (DAPI, fluorescein and rhodamine) for a total of 18 acquired images per well. Images were segmented and analysed with CellProfiler cell image analysis software. The imaging pipeline used to segment the images is available on request. Cell morphology and intensity data were acquired on a per image and per cell basis, and exported into a mySQL database. The data were visualized with SpotFire (TIBCO) and CellProfiler Analyst.

Immunofluorescence microscopy. U2OS cells were plated on number 1 glass coverslips (VWR) and were cultured in DMEM + Pen/Strep + 10% v/v FBS (complete media) at 37 °C in a 5% CO_2 atmosphere, then exposed to 10 Gy ionizing radiation from a ^{137}Cs source in a Gammacell irradiator (Atomic Energy of Canada), fixed in methanol and processed for immunofluorescence using the antibodies indicated above. Images were captured on a Zeiss Axiophot II microscope with a Hamamatsu CCD (charge-coupled device) camera and processed with OpenLab/Volocity software. We used CellProfiler (www.CellProfiler.org) or ImageJ software (http://rsb.info.nih.gov/nihimageJ) for quantitative image analysis.

RT–PCR. Total RNA was extracted from 10^6 U2OS cells expressing either control or Brd4-directed shRNA, with an RNeasy kit (Qiagen). Complementary DNA was generated with oligo(dT) primers with SuperScript reverse transcriptase (Invitrogen) according to the manufacturer's instructions. These complementary DNAs were used as templates for linear-range PCR amplification or quantitative real-time PCR with SYBR green master mix on an Applied Biosystems 7500 with the following primers: forward 5′-CTC CTC CTA AAA AGA CGA AGA-3′ and reverse (pan-Brd4 isoform) 5′-TTC GGA GTC TTC GCT GTC AGA GGA G-3′, (Brd4 isoform A) 5′-GCC CCT TCT TTT TTG ACT TCG GAG C-3′, (Brd4 isoform B) 5′-GCC CTG GGG ACA CGA AGT CTC CAC T-3′, (Brd4 isoform C) 5′-CCG TTT TAT TAA GAG TCC GTG TCC A-3′, (CHEK2) forward 5′-ACAGATAAATAC CGAACATACAGC-3′ and reverse 5′-GACGGCGTTTTCCTTTCCCTACAA-3′, and using (GAPDH) primers forward 5′-GATGCCCTGGAGGAAGTGCT-3′ and reverse 5′-AGCAGGCACAA CACCACGTT-3′ as control for normalization.

Expression profiling and analysis. Total RNA was collected from stable U2OS cells expressing Brd4 or control shRNA using RNeasy (Qiagen), labelled and analysed on the Affymetrix U133 Plus 2.0 array. Unsupervised clustering of expression data was performed using the R package pvclst. LIMMA[21] was used to identify important changes in expression between Brd4 knockdown and control cells. Data were deposited in the US National Institutes of Health Gene Expression Omnibus (http://www.ncbi.nlm.nih.gov/geo/query/acc.cgi?acc=GSE30700).

Subcellular fractionation. U2OS cells expressing Flag-tagged Brd4 isoforms were lysed in hypotonic conditions (10 mM Hepes, 10 mM NaCl, 25 mM KCl, 1 mM $MgCl_2$, 0.1 mM EDTA, pH 7.4 with protease inhibitors) and subjected to flash freezing in liquid nitrogen 1 h after mock treatment or exposure to 10 Gy of ionizing radiation with a ^{137}Cs source in a Gammacell irradiator (Atomic Energy of Canada). Cells were thawed at room temperature and spun down at 10,000*g* for 10 min. The supernatant was saved as the cytoplasmic fraction and concentrated down using trichloroacetic acid precipitation and reconstituted in 2× Laemmli buffer. The pellet was re-suspended in high salt buffer (20 mM Hepes, 0.5 mM DTT, 1.5 mM $MgCl_2$, 0.1% Triton X-100, 1 M NaCl, pH 7.4 with protease inhibitors) and left on ice for 30 min followed by a high-speed spin at 100,000*g* for 30 min. The supernatant was saved as the high salt fraction and concentrated down using trichloroacetic acid precipitation and reconstituted in 2× Laemmli buffer. Sulphuric acid (0.4 N) was added to the high-speed pellet and left on ice for 30 min, followed by a high-speed spin at 14,000*g* for 10 min. The supernatant was saved as the acid fraction and concentrated down using trichloroacetic acid precipitation and reconstituted in 2× Laemmli buffer.

Western blotting and immunoprecipitation. Cells were treated with 10 Gy ionizing radiation with a ^{137}Cs source in a Gammacell irradiator (Atomic Energy of Canada). For whole cell lysates, cells were trypsinized and lysed in LB (4% SDS, 120 mM Tris, pH 6.8) with protease and phosphatase inhibitors (Complete mini EDTA-free and PhosSTOP, Roche Applied Science). For chromatin isolation, cells were trypsinized, re-suspended in low salt buffer (LSB: 10 mM Hepes 10 mM NaCl, 25 mM KCl, 1.0 mM $MgCl_2$, 0.1 mM EDTA, pH 7.4 + protease inhibitors, as above), flash-frozen in liquid N_2, thawed, pelleted at 10,000*g* for 10 min, re-suspended in high salt buffer (HSB: 20 mM Hepes, 1.0 M NaCl, 0.5 mM DTT, 1.5 mM $MgCl_2$, 0.1% Triton X-100 + protease inhibitors) for 45 min on ice, pelleted at 100,000*g* for 30 min., and proteins from the supernatant were precipitated with trichloroacetic acid. For immunoprecipitation, U2OS cells expressing Flag-tagged Brd4 isoforms were lysed in low salt buffer (50 mM Tris HCl, pH 7.4, 150 mM NaCl, 1 mM EDTA, 0.5% NP-40 with protease inhibitors) and subjected to flash freezing in liquid nitrogen 1 h after mock treatment or irradiation. Cells were thawed at room temperature and spun down at 10,000*g* for 10 min. The supernatant was removed and saved as the pre-immunoprecipitation cytoplasmic fraction. The nuclear pellet was re-suspended in low salt buffer, tip sonicated at 4 °C (35% amplitude, pulse 5 s on and off for three cycles), and spun down at

14,000*g* for 10 min. The supernatant was collected as starting material for immunoprecipitation using M2 Flag beads (Sigma Aldrich) overnight at 4 °C. The beads were then spun down and the first supernatant saved as the unbound fraction. The beads were washed five times with low salt buffer and proteins were solubilized in 2× Laemmli buffer and boiled at 95 °C for 3 min before loading onto SDS–PAGE. Samples were processed after SDS–PAGE for gel band cutting and in gel tryptic digestion for mass spectrometry or western blotting to detect pulldown of the condensin II complex (SMC2 and SMC4 proteins) with Brd4 isoforms. SDS–PAGE and western blot was according to the methods of Laemmli and Towbin using either a Li-cor Odyssey scanner or horseradish-peroxidase-coupled secondary antibodies (Bio-Rad) and Western Lightning enhanced chemiluminenscene (PerkinElmer) for visualization of bands.

Pulsed-field gel electrophoresis and micrococcal nuclease assay. For pulsed-field gel analysis, control and BRD4 knockdown cells were plated at 1×10^6 cells per plate, exposed to 10 Gy ionizing radiation with a ^{137}Cs source in a Gammacell irradiator (Atomic Energy of Canada) and collected at 0.5, 1, 2, 3 and 5 h. Cells were trypsinized, diluted to 2×10^6 cells and embedded in agarose plugs. The agarose plugs were exposed to Proteinase K (1 mg ml^{-1}) in 500 mM EDTA, 1% N-lauryl Sarcosyl, pH 8.0, for 48 h, washed 3 × 1 h with TE buffer, loaded onto a 0.675% agarose gel and separated under pulsed-field conditions with a Rotaphor 6.0 (Biometra). Nuclei from control and Brd4 knockdown cells were isolated by hypotonic lysis and micrococcal nuclease assays performed as described by Carey and Smale[22].

Flow cytometry. U2OS cells were plated and transiently transfected GFP transgenes or siRNA as indicated, exposed to varying doses of ionizing radiation from a ^{137}Cs Gammacell irradiator source (Atomic Energy of Canada) and collected at varying times as indicated by fixation with 4% formaldehyde (cell-death measurements) or directly extracted with 100% ethanol (cell-cycle measurements), and processed for flow cytometry using the antibodies listed above. Data were analysed using FlowJo (www.flowjo.com) software.

Colony formation assays. Control and BRD4 knockdown cells were exposed to the indicated doses of ionizing radiation from a ^{137}Cs source in a Gammacell irradiator (Atomic Energy of Canada), or left untreated, trypsinized, counted and re-plated using serial dilutions. Colonies were propagated to the 10- to 15-cell stage (3–7 days), stained with Wright stain (Sigma) and counted with CellProfiler software or by averaging counts of ten fields from three independent observers using a dissection microscope to identify colonies of more than 15 cells.

Constructs, shRNA and siRNA, and transfection. Full-length constructs of Brd4 Isoform A (accession number NM_058243), B (accession number BC035266) and C (accession number NM_014299.2) were cloned into pEGFP-C1 (Clontech) and pFLAG-CMV2 (Sigma) by PCR. Bromodomain mutations were introduced using quickchange (Stratagene) using PCR primers: 5′-AAA TTG TTA CAT CGC CAA CAA GCC TGG AGA TGA CGC AGT CTT AAT GGC AG-3′ and 5′-CTG CCA TTA AGA CTG CGT CAT CTC CAG GCT TGT TGG CGA TGT AAC AAT TT-3′. Cells were transfected with Fugene 6 (Roche) according to the manufacturer's instructions. shRNA directed against Brd4 were from the TRC library (see Supplementary Table 1), or created in the mir30-based pMLP vector (a gift from M. Hemann) with primer 5′-TGC TGT TGA CAG TGA GCG AAG ACA CA-3′ for Brd4. U2OS cell lines stably expressing this shRNA or control hairpins (ineffective hairpins directed against human sequences of BAD and PUMA) were created using puromycin selection at 2 μg ml^{-1}. STEALTH siRNA against pan-isoform BRD4, SMC2 and control were purchased from Invitrogen. Custom Brd4 isoform-specific siRNA were synthesized from Dharmacon using the following sequences: isoform A specific 5′-GGG AGA AAG AGG AGC GUG AUU-3′ and isoform B specific 5′-GCA CCA GUG GAG ACU UCG UUU-3′. siRNA against SMC2 was from Dharmacon. For siRNA experiments, cells were transfected with Lipofectamine RNAiMax (Invitrogen) according to the manufacturer's instructions.

Mass spectrometry. Proteins from the Brd4 co-immunoprecipitation were examined after SDS–PAGE by staining with Coomassie blue. Gel bands were excised, de-stained and processed for digestion with trypsin (Promega; 12.5 ng μl^{-1} in 50 mM ammonium bicarbonate, pH 8.9). Peptides were loaded directly onto a column packed with C18 beads. The column was placed in-line with a tapered electrospray column packed with C18 beads on a Orbitrap XL mass spectrometer (Thermo Scientific). Peptides were eluted using a 120-min gradient (0–70% acetonitrile in 0.2 M acetic acid; 50 nl min^{-1}). Data were collected using the mass spectrometer in data-dependent acquisition mode to collect tandem mass spectra and examined using Mascot software (Matrix Science).

Network analysis. Protein–protein and kinase–substrate interactions relevant to DNA damage signalling were hand curated from primary literature available in PubMed using the initial keywords 'DNA damage', 'cell cycle checkpoint', 'chromatin structure', 'ATM/ATR', 'Chk1/Chk2' and 'SMC proteins', and following reference lists.

21. Smyth, G. K. Linear models and empirical bayes methods for assessing differential expression in microarray experiments. *Stat. Appl. Genet. Mol. Biol.* **3,** Article3 (2004).
22. Carey, M. & Smale, S. T. Micrococcal nuclease-Southern blot assay: I. MNase and restriction digestions. *CSH Protoc.* **2007**, http://dx.doi.org/10.1101/pdb.prot4890 (2007).